REPAIR TECHNOLOGIES OF MECHANICAL DRIVE STEAM TURBINES FOR CATASTROPHIC DAMAGE

by

Manabu Saga

Manager, Turbine Design Section

Shugo Iwasaki

Acting Manager, Materials Laboratory

Yuzo Tsurusaki

Mechanical Engineer, Turbine Design Section

and

Satoshi Hata

Manager, Turbine Design Section

Mitsubishi Heavy Industries, Ltd.

Hiroshima, Japan

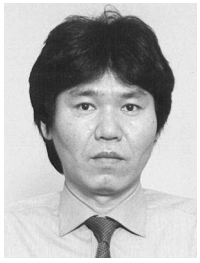

Manabu Saga is a Manager of the Turbine Design Section in the Turbomachinery Engineering Department, Mitsubishi Heavy Industries, Ltd., in Hiroshima, Japan. He has had experience with basic and detail engineering of steam turbines and gas turbines for power generation and development.

Mr. Saga has a B.S. degree (Mechanical Engineering) from Keio University.

Shugo Iwasaki is Acting Manager of the Materials Laboratory in the Hiroshima Research and Development Center, Mitsubishi Heavy Industries, Ltd., in Hiroshima, Japan. He has 12 years of experience in the evaluation of materials, the development of new manufacturing processes, and troubleshooting for turbines, compressors, heat exchangers, and vessels.

Mr. Iwasaki has B.S. and M.S. degrees (Materials Engineering) from Kyushu University.

Yuzo Tsurusaki is the Mechanical Engineer of the Turbine Design Section in the Turbomachinery Engineering Department, Mitsubishi Heavy Industries, Ltd., in Hiroshima, Japan. He is a specialist in rotor design and has five years of experience with troubleshooting of steam turbines.

Mr. Tsurusaki graduated from Kurume College of Technology (Mechanical Engineering).

ABSTRACT

Mechanical drive steam turbines play an important role as core equipment in petrochemical plants, and these turbines are protected for safe operation by an antioverspeed trip device, as well as other monitoring and protection systems. However, in some cases, a turbine will suffer severe mechanical damage due to improper operation or failure to activate the protection system as a result of human error. For urgent plant recovery and to minimize the duration of risky operation with no spare rotor, a damaged turbine has to be repaired in as short a time as possible. This paper introduces actual experiences in repairing and reviving catastrophically damaged turbine rotors through special welding procedures, based on element tests to find the optimized welding conditions, detailed strength calculations to confirm the integrity, and heat transfer analysis for proper heat treatment process conditions. These basic procedures are discussed to show useful data. The revived rotor of the extraction condensing turbine was placed back into the casing and operated. The turbine was uniquely modified in order to balance the required amount of power and minimize the repair time, to restart the plant as quickly as possible. The case study for this optimization is discussed by showing thermodynamic calculations, performance, and repair schedules.

Root cause analysis for the process of the catastrophic failure is explained, for the integrated control system governing the control and operation positioner systems.

INTRODUCTION

Mechanical drive steam turbines play important roles in petrochemical plants. For safety in operation, these turbines are protected by an overspeed trip device, as well as other monitoring and protection systems. However a turbine still can suffer severe mechanical damage from improper operation or failed activation of protection systems, caused by human error and improper control of steam purity.

When rotor damage does occur, a rotor is normally replaced with a spare rotor and the plant continues to operate with the running risk of having no replacement rotor. For urgent plant recovery and to minimize the operating time with no spare rotor, a damaged turbine has to be repaired in as short a time as possible. However, in cases where the damage is catastrophic and existing technology cannot repair the damaged rotor, it has to be scrapped and a new rotor must be fabricated. Consequently, the end user has to wait a minimum of six months to one year for a new rotor.

In order to repair and revive a catastrophically damaged turbine rotor in emergencies in response to end user requirements, a new welding technique has been developed based on risk analysis of repair and laboratory element tests. In addition, to optimize welding conditions, the authors studied detailed strength calcula-

tions to confirm integrity, and performed heat transfer analysis for finding proper heat treatment process conditions.

The authors introduce typical experiences in rotor repair by discussing useful results of the above analysis and the test results.

FAILURE MODE OF STEAM TURBINES

The failure damage modes of mechanical steam turbines are classified into main components for steam flow paths, rotating components such as rotors, grooves, disks, and blades, as well as stationary parts such as control valve bearings (Table 1). The basic root causes for each damage mode are listed. Severe damage modes include destruction of blades due to excessive centrifugal force, blade corrosion fatigue failure, and rotor bowing due to interference/rubbing in transient operations such as initial start up.

Table 1. Failure Damage Mode.

Components		Damage Mode	Root Causes
Flow Path Parts	Control Valve	Valve Stem Bending Fatigue Failure	High Steam Velocity Fluid Excitation
	Nozzles (HP)	Solid Particle Erosion Fouling	Hard Foreign Materials Inside of Pipes
	Blades (HP)	Solid Particle Erosion Fouling	Hard Foreign Materials Inside Steam Impurity
	Nozzles (LP)	Fouling	Steam Impurity
	Blades (LP)	Drain Attack Erosion Fouling	High Moisture & High Velocity Steam Impurity
Rotating Parts	Blades (HP)	High Cycle Fatigue Failure Centrifugal Force Failure	Excessive Excitation Force Excessive Over Speed
	Blades (LP)	High Cycle Corrosion Fatigue Centrifugal Force Failure	Improper Water Treatment Excessive Over Speed
	Rotor	Rubbing & Shaft Bow & High Vibration Disk SCC	Improper Start Up Drain Intake, Steam Impurity
	Thrust Collar Journal Shaft	Rubbing & Scratch/Wear	Excessive Thrust Force Improper Oil Supply (UPS)
	Bearings	Rubbing & Melting	Excessive Thrust Force Improper Oil Supply (UPS)
Stationary Parts	Casing	Creep Deformation/ Creep Rapture, Erosion/Corrosion	Operation Over Allowance Excessive Drain / Galvanic
	Diaphragm	Diaphragm Bending Deformation Erosion & Corrosion	Operation Over Allowance Excessive Drain / Galvanic
	Seals	Rubbing & Erosion	Improper Start Up Excessive Drain

In Figure 1, a typical damage condition is shown in the steam turbine cross section. The first stage nozzle profiles are eroded at the trailing edges, due to contact with hard solid particles. The flow path of the diaphragm and blade profiles at the leading edges in the low-pressure (LP) high moisture section are eroded by water droplets. In some cases, the welded zone of the nozzles are affected by a combination of erosion and corrosion. Corrosion fatigue failure will occur in the blades of the LP section at the wet and dry enrichment zone under corrosive conditions, if proper water treatment is not performed during steady and transient operation, or if a corrosive chemical leakage occurs at a heat exchanger. Excessive contact friction at the rotor thrust collar will induce melting damage of thrust bearing pads, due to excessive thrust force from drain invasion. In other cases, lubricant oil additives may generate oil sludge contaminants on pad lubricating surfaces, and this will reduce bearing durability. If lubricant oil is not selected properly, in the worst case the rotor will rub against the bearings.

TYPICAL FAILURE EXPERIENCE

Rotational equipment manufacturers design, manufacture, and deliver steam turbines to customers based on well-proven technologies and supply experiences, and therefore they do not experience catastrophic accidents. However, this paper introduces typical catastrophic damage in using steam turbines.

Figure 2 shows trends in rotation speed and key events from start to excess speed rotor damage, during the site-based solo running test. This extraction condensing turbine for driving a charge gas compressor is equipped with a position control backup system. The turbine was coasted up smoothly to a maximum continuous speed of maximum continuous rate (MCR) 10,279 rpm. Rotating speed was increased for a moment to electric overspeed trip speed (EOST); however, the trip interlock did not activate and speed

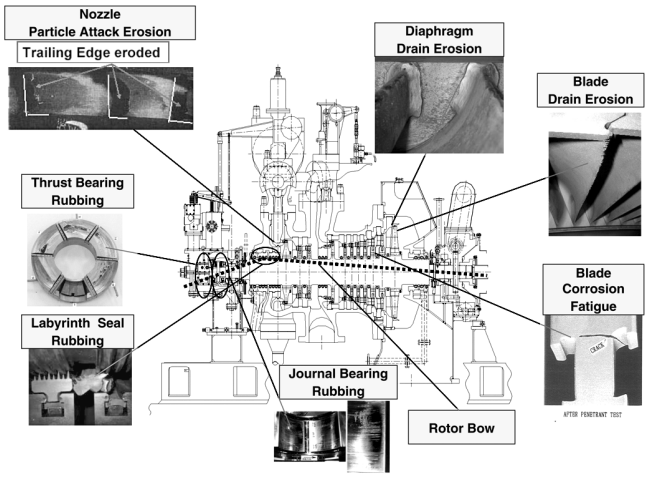

Figure 1. Failure Damage Map.

continued to increase, exceeding EOST speed. After the operating governor function key and the turbine control were shifted to the backup system, the governing valve suddenly opened from 12 percent to 60 percent in a no load condition and the turbine rotor was accelerated to 170 percent of MCR. Eventually, the turbine rotor disks and blades became damaged, resulting in oil leakage.

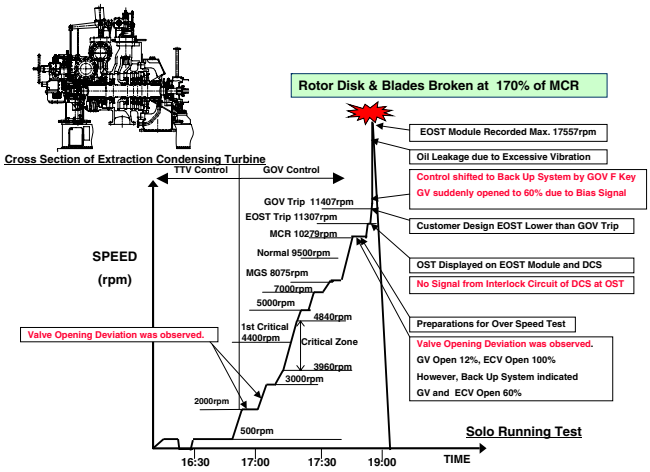

Figure 2. Typical Failure Experience (Overspeed Burst).

The control system for this turbine is shown in Figure 3. The control system has backup modules operating by position control, and this position control is used to supply the actuator output signal instead of the electric governor in the case of a governor failure. The backup system monitors the actuator output signals from the governor and controls two signals to switch the actuator signal source from governor to position control. Two backup modules are utilized for governing and extraction control valve actuators.

As a result of detailed investigation of the system and signals, it was found that circulating current from the distributed control system (DCS) into the signal system of the backup modules caused the supply signal to the actuator to increase, thereby opening the valve. This caused a large amount of steam flow leading to the abnormal increase in rpm, and the interlock that should have performed an emergency valve close did not operate properly.

Circulating current causes a 12 percent to 60 percent deviation of signals between the governor and governor backup module.

The actual damage conditions are shown in Figure 4 and Figure 5. The second (high-pressure section) and third stage blades (low-pressure section) have broken off from the rotor grooves, and the disks and grooves are deformed at the first stage and other stages

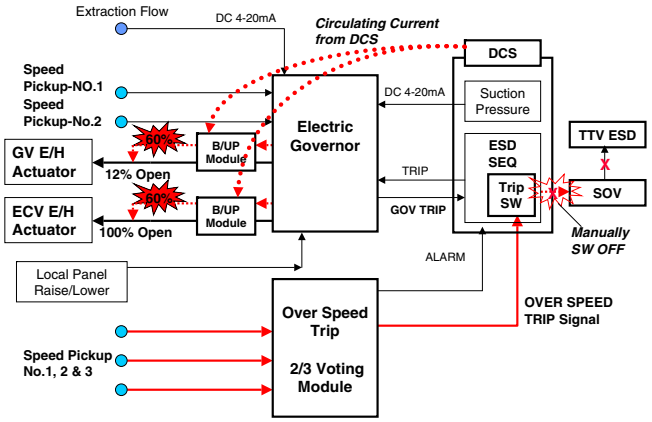

Figure 3. Overspeed Burst and Back Up System Error.

of the low-pressure section. The rotor is bowed from a large amount of friction and contact due to a seriously unbalanced condition. The journal and thrust bearings are damaged and their Babbitt metal pad has melted due to a huge friction loss heating resulting from the excessive overspeed and high loads. Rotor shaft at bearing location had no damage and was protected by Babbitt metal melting promptly. As explained in Figure 5, damage of the rotor was catastrophic.

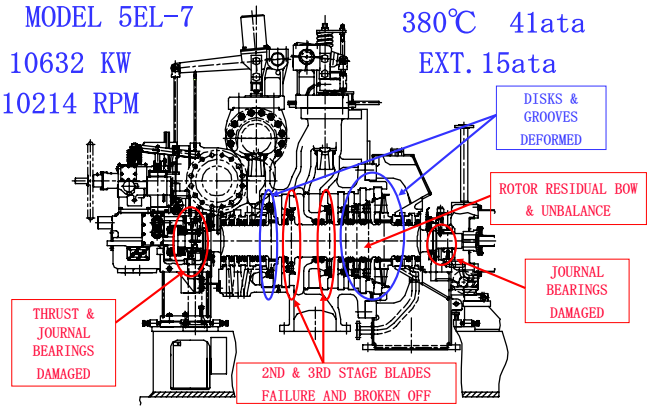

Figure 4. Damaged Condition of Turbine.

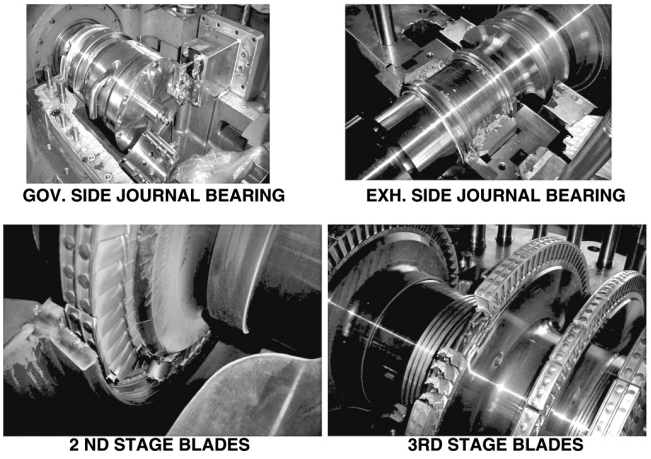

Figure 5. Detail Damaged Condition of Turbine.

REPAIR RISK ANALYSIS

For urgent plant recovery and to minimize the duration of operation with no spare rotor, this damaged rotor had to be repaired in as short a time as possible. In order to revive this catastrophically damaged turbine rotor, a special welding procedure was necessary.

In order to analyze the applicability of overlay welding for this turbine, technical risks are evaluated in a common procedure for rotor repair according to experiment data. In addition, experience with welding rotors and risk factors are categorized as well-proven, possible, practical, or not well-proven. Table 2 shows details of this test.

Table 2. Technical Risk Evaluation.

Risk Factor		Evaluation	Results/Countermeasures
Element for Welding	Mechanical Properties Deterioration	2.25Cr-1Mo Welded Metal Lab. Test Stress of Damaged Parts Change of Impact Value and others	8% Decrease of Tensile Strength Proper Safety Factor of Yield Stress
	Creep Strength	10% Decrease is Expected from Mech. Property and Temp. Test	Proper Safety Factor of Creep Life Expected 300 to 400℃
	SCC Strength	Confirmed by SCC Test.	NO SCC
	Residual Stress	Residual Stress is Measured by Test and Actual Rotor..	Within Allowable
	Welding Procedure	Applied for Test and Actual Rotors including Heat Treatment & NDE.	WPS/PQR Issued
	Cold Cracking	Well-Proven Heat Treatment Procedure Heat Transfer Analysis for Disks Circumferential Equal Temperature Profile	Issued Basic Procedure is OK Heat Transfer Analysis is Required.
	Stress Relief Cracking		
	Blow Holes Defects	Applied for Test and Actual Rotors including Heat Treatment & NDE.	WPS/PQR Issued
	Residual Deformation Spring Back	Applied for Actual Rotors and Within Criteria 0.005mm for Disks. No Experience for HP Balance Piston	Basically Expected Within Criteria Stress Analysis & Actual Size Test are Required.
	Eccentricity & Unbalance	By Fine Setting and Machining After Welding & Balancing, They Can Be Within Criteria.	Actual Size Test are Required for Damaged Parts.
Element for Operation	Rubbing Spiraling vs Bonding Stress	Confirmed Same Bonding Strength By Lab. Test Deformation due to Stress Relief by Contact Heating	Stress Relief and No Spring Back during operation to be confirmed by Actual Size Test
	Long Term Capability	No Impacts for Creep, SCC by Test and For Corrosion Fatigue due to HP Sect.	Stress Relief and No Spring Back during operation to be confirmed by Actual Size Test
Element for Experience	Welded Position	No Experience for HP Balance Piston	Actual Size Test are Required.
	Boundary Condition	Experience of HP and LP stage Disks	Expected 300 to 400℃ Heat Transfer Analysis is Required.
	Unexpected Defects	Applied for Test and Actual Rotors including Heat Treatment & NDE.	No Blowhole Inspected

Elements of welding risk factors include mechanical properties, creep and SCC strength, residual stress, cold cracking, and residual deformation of the rotor. Risks in operation after repair consist of the bonding strength in frictional areas and spiraling around the labyrinth seal at the high temperature and pressure side.

For the risk analysis and evaluation, element tests were performed to find the optimum welding conditions, detailed strength calculations were performed to confirm the integrity, and heat transfer analysis was performed to achieve proper heat treatment process conditions. These basic procedures are studied and discussed in the next section.

As explained below, mechanical properties and strength can be maintained at the same levels as that of a new rotor. However, residual rotor deformation is affected by residual stress in the surface of the welded shaft section. This deformation must be less than 0.005 mm (.0002 inch) when considering required limit criteria for balance. Though it is possible to calculate residual stress and shaft deformation, it is very difficult to predict such a small amount of deformation precisely.

Because of this, residual warpage of the rotor still remains as a risk factor, and an actual full scale test is necessary to confirm that residual warpage is within allowances, and that there are no changes when reheated.

TECHNIQUES FOR WELD REPAIR

Technical Issues and Solutions for Weld Repair

Table 3 summarizes the technical issues on weld repair of damaged rotor disks and solutions for those issues. The rotor shaft at the bearing has no damage and was protected by the Babbitt metal melting promptly. Damaged pads can be easily replaced with spare pads. However, there are risks in replacing forged rotor material with weld deposited material. Forging gives the rotor material proper mechanical properties and reduces defects caused by casting, but weld repairs have no such effects. Therefore, it is necessary to apply welding material that will provide proper mechanical properties even though there is no forging in the repair process. The proper welding material was selected as explained in the following section.

Table 3. Technical Issues and Solutions on Weld Repair of Damaged Rotor Disk.

Technical issues	Process	Solution	Check points on test	
			Lab. scale	Real scale
•Properties of weld metal	-	•Proper material selection	-	-
•Welding defects	Welding	•Same allowable defect size for weld metal with base metal	G H	G H
•Deformation	Welding PWHT	•Uniform heat input •Local heating •Uniform heat input •Vertical rotor layout	-	A
•Residual stress	(Local) PWHT	•Optimum heater layout based on FE analysis	-	F
•Reduction of strength on base metal •High hardness on HAZ	PWHT	•Proper heating temperature and time	B C D E	C

A: dimension measurement B: Tensile test C: Hardness measurement D: Impact test
E: SCC test F: Residual stress measurement G: Ultrasonic test H: Magnetic particle test

Proper welding methods and conditions should be provided to avoid welding defects that would initiate cracks. Proper welding conditions were decided by welding laboratory scale test pieces. An ultrasonic test for the weld metal was performed with the same criterion on minimum defect size as for the base rotor metal.

Temperature distribution and gravity during welding and post weld heat treatment (PWHT) cause unfavorable deformation in the rotor. Therefore, the repaired disk was heat treated locally, and the rotor was suspended vertically at the PWHT to prevent bowing of the shaft. The whole circumference of the repaired disk was welded and heat treated uniformly.

The welded portion needs to be heat treated to reduce residual stresses due to welding and hardening at the heat affected zone (HAZ), which can cause stress corrosion cracks (SCC) under wet conditions. However, PWHT reduces the strength of base metal and weld metal. Therefore, the repaired disk was heat treated locally to avoid degradation of the base metal. An optimum PWHT temperature satisfying both weld metal strength and HAZ hardness was determined.

Selecting Weld Metal

Ni-Mn-Mo steel (AWS:ER110S-G) and 2.25Cr-1Mo steel (AWS:ER90S-G) were proposed as the welding material because of their excellent welding characteristics, strength, and toughness. Table 4 shows the comparison of these material properties. Ni-Mn-Mo steel is suitable as weld metal for the disk that requires high strength at lower temperatures. However, 2.25Cr-1Mo steel is suited for higher temperatures because of its creep strength. The latter is preferable because it can be utilized for the entire rotor stage. Thus 2.25Cr-1Mo steel was ultimately selected as the metal for repair welding. Both materials were welded and evaluated in testing conducted on a laboratory scale test.

Table 4. Weld Metal for Repair.

Required Properties	2.25Cr-1Mo steel (AWS:ER90S-G)	Ni-Mn-Mo steel (AWS:ER110S-G)
Tensile strength	OK	OK
Creep strength	OK	NG
Toughness	OK	OK
Durability for SCC	OK	OK
Weldability	OK	OK
Applicable object	High/Low temperature stage	Low temperature stage

Welding and Post Weld Heat Treatment on a Laboratory Scale Test Piece

Figure 6 shows the appearance of the test piece after welding. Both types of weld material were welded to a bar shaped rotor material (1.25Ni-Cr-Mo steel). The weld metal was formed with a thickness of 75 mm (2.95 inches) on the bar by gas tungsten arc welding (GTAW). Optimum welding conditions were selected to avoid defects and these were controlled constantly throughout the welding process to obtain uniform heat input to the bar. Table 5 shows the welding and PWHT conditions for the test pieces.

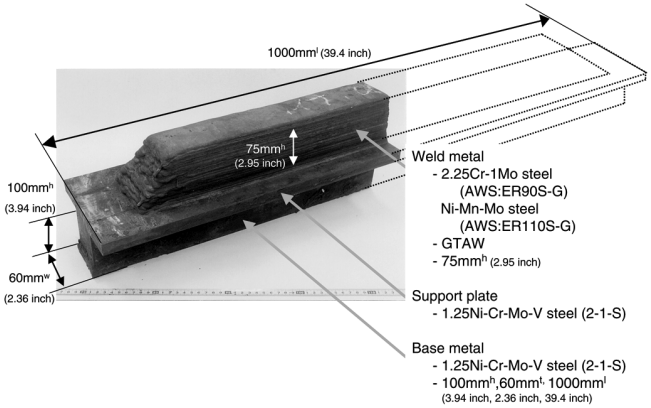

Figure 6. Appearance of Welded Test Piece in Laboratory Scale Test.

Table 5. Welding and PWHT Conditions for Test Pieces.

Weld metal		2.25Cr-1Mo steel	Ni-Mn-Mo steel
Preheating		150-250 °C (302-482°F)	←
Welding	Current	200-300 A	←
	Voltage	11-16 V	←
	Traveling speed	6-7 cm/min (2.4-2.8 inch/min)	←
Postheating		250-300 °C (482-572°F), 1h	←
PWHT (Furnace heating)	Heating	20 °C/h (36°F/h)	←
	Holding	-585 °C (1085°F), 10h -600 °C (1112°F), 10h	-600 °C/h (1112°F), 10h
	Cooling	25 °C/h (45°F/h) to 250 °C (482°F/h) →Air cooling	←

Figure 7 shows the relationship between stress and time to SCC initiation reported by Speidel and Bertilsson (1984). Based on these data, it is estimated that the critical stress that causes SCC after 105 hours of operation is 420 MPa in a normal steam environment. Considering the safety factor, the target residual stress on the weld metal was set at 200 MPa.

The specimens for evaluation were taken in a welded condition and the heat treated test pieces. Figure 8 indicates the locations of each specimen in the test piece. Tensile, impact, hardness measurement, microstructure observation, and SCC tests were performed.

Evaluation of Laboratory Scale Test Pieces

Welding Defects

Welded test pieces were inspected by ultrasonic testing. Defects exceeding the criteria [1.6 mm (.06 inch) in diameter] were not found. According to the analysis by fracture mechanics, the critical defect size for cracking is much larger then the criterion. Therefore, it can be concluded that the defect in weld was small enough to prevent fracture.

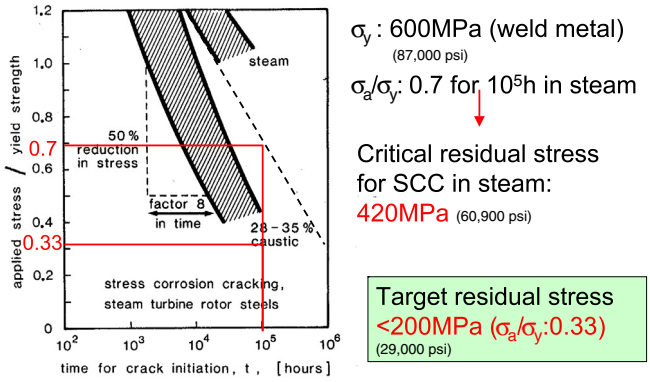

Figure 7. Estimated Critical Residual Stress for SCC. (Courtesy Speidel and Bertilsson, 1984)

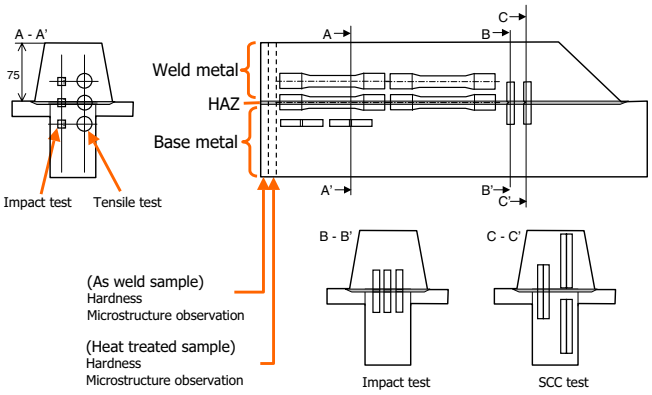

Figure 8. Locations of Specimens for Evaluation.

Mechanical Properties

Table 6 shows results of the mechanical tests on test pieces welded using 2.25Cr-1Mo steel and heat treated for 10 hours at 585°C and 600°C (1085°F and 1112°F). Figure 9 and Figure 10 indicate distribution of hardness on the welded test piece and the heat treated piece at 600°C (1112°F).

Hardness, tensile properties, and impact value on both heating temperatures satisfied the target for the weld metal and the requirement for base metal, except for hardness heated at 585°C (1085°F). Figure 11 shows the relationship of maximum hardness and minimum tensile strength with PWHT temperature. Hardness and tensile strength of the weld metal tends to become weaker as the welding temperature becomes higher. On the other hand, tensile strength of base metal is almost constant in the temperature range tested. This tendency comes from the high temperature properties of base metal.

The maximum hardness of HAZ satisfies the target at lower temperatures. On the other hand, the minimum tensile strength of the weld metal satisfies the target at higher temperature. Therefore, temperature range that satisfies both targets is between 595°C and 600°C (1103°F and 1112°F) when welding with 2.25Cr-1Mo steel.

Table 7 shows the results of mechanical tests for a test piece welded with Ni-Mn-Mo steel. The tensile strength of Ni-Mn-Mo weld metal is higher than the one of 2.25Cr-1Mo heat treated at the same time and at the same temperature [10 hours, 600°C (1112°F)]. This shows that the Ni-Mn-Mo weld metal has an advantage in strength over 2.25Cr-1Mo at low temperatures.

Sensitivity for Stress Corrosion Cracking

An SCC test was performed in an accelerating NaCl solution for the test piece, for the 2.25Cr-1Mo weld metal. Table 8 shows the test conditions. Figure 8 shows the location of specimens on the test piece. Stress around the yield point of material was applied by U-bending. The surface of the test pieces was observed up to 1000 hours.

Figure 12 indicates the appearance of the HAZ specimen after the 1000 hour test. Although the surface became rough by corrosion, cracks did not occur.

Table 6. Mechanical Properties of Specimens (Weld Metal: 2.25Cr-1Mo Steel).

		585°C (1085°F), 10h			Target for weld metal
		Base metal	HAZ	Weld metal	Requirement for base metal
Vickers hardness, HV	Max	324	370	286	350
	Min	277		243	
Tensile strength MPa (psi)		927 (134,500) 922 (133,700)	938 (136,000) 971 (140,800)	793 (115,000) 792 (114,900)	720 (104,400) { 785 (113,900) }
Yield strength MPa (psi)		785 (113,900) 785 (113,900)	817 (118,500) 850 (123,300)	645 (93,500) 642 (93,100)	600 (87,000) { 638 (92,500) }
Elongation %		23.2 23.2	24.0 23.2	28.0 28.0	15 { 15 }
Reduction of area %		66.5 66.5	68.9 64.0	71.3 69.7	40 { 40 }
Charpy 2mm (0.08inch) U Notch J (ft-lbf)	Longitudinal direction	77 (57) 112 (83)	191 (141) 201 (148)	201 (148) 153 (113)	39 (29) { 39 (29) }
	Thickness direction	-	87 (64) 98 (73) 67 (50)	-	

		600°C (1112°F), 10h			Target for weld metal
		Base Metal	HAZ	Weld metal	Requirement for base metal
Vickers hardness, HV	Max	297	339	309	350
	Min	262		210	
Tensile strength MPa (psi)		932 (135,200) 951 (137,900)	913 (132,400) 921 (133,600)	722 (104,700) 725 (105,200)	720 (104,400) { 785 (113,900) }
Yield strength MPa (psi)		791 (114,700) 812 (117,800)	795 (115,300) 808 (117,200)	602 (87,300) 602 (87,300)	600 (87,000) { 638 (92,500) }
Elongation %		22.5 22.5	24.5 24.0	28.5 28.5	15 { 15 }
Reduction of area %		66.5 66.5	69.7 68.2	74.3 74.3	40 { 40 }
Charpy 2mm (0.08inch) U Notch J (ft-lbf)	Longitudinal direction	91 (67) 143 (106)	83 (61) 99 (73)	229 (169) 197 (145)	39 (29) { 39 (29) }
	Thickness direction	-	83 (61) 94 (69) 99 (73)	-	

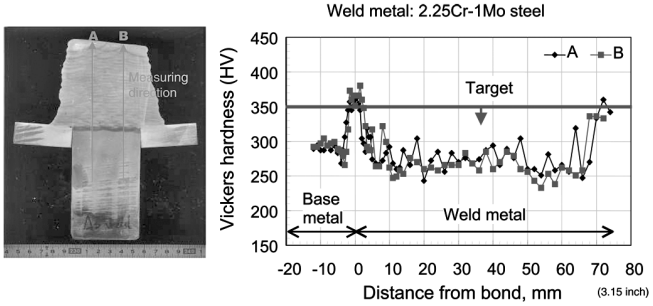

Figure 9. Distribution of Hardness on Welded Test Piece.

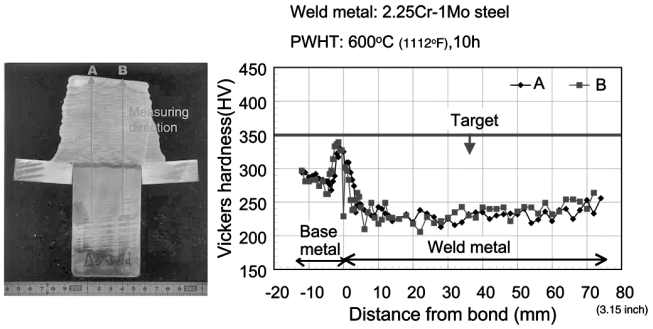

Figure 10. Distribution of Hardness on Heat Treated Test Piece.

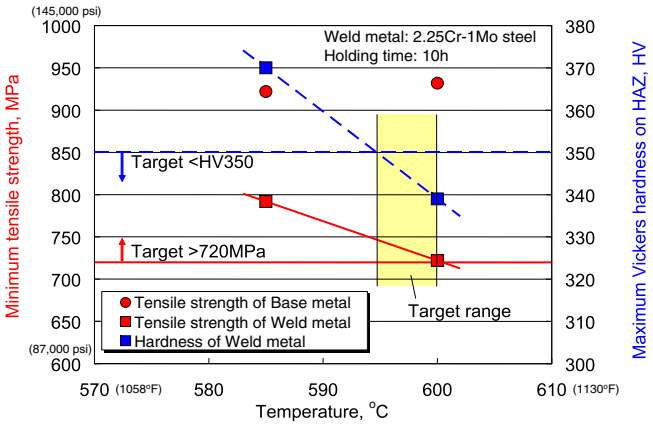

Figure 11. Relationship Between PWHT Temperature and Mechanical Properties.

Table 7. Mechanical Properties of Specimens (Weld metal: Ni-Mn-Mo Steel).

		600°C (1112°F), 10h			Target for weld metal
		Base metal	HAZ	Weld metal	Requirement for base metal
Vickers hardness, HV	Max	313	340	315	350
	Min	292		280	
Tensile strength MPa (psi)		932 (135,200) 932 (135,200)	921 (133,600) 928 (134,600)	858 (124,400) 852 (123,600)	720 (104,400) [785 (113,900)]
Yield strength MPa (psi)		796(115,500) 799(115,900)	828 (120,100) 826 (119,800)	766 (111,100) 776 (112,500)	600 (87,000) [638 (92,500)]
Elongation %		24.6 24.0	24.2 23.0	27.8 28.4	15 [15]
Reduction of area %		68.9 68.2	64.8 68.2	67.3 69.7	40 [40]
Charpy 2mm (0.08inch) U Notch J (ft-lbf)	Longitudinal direction	180 (133) 179 (132)	196 (145) 178 (131)	130 (96) 138 (102)	39 (29) [39 (29)]
	Thickness direction	-	96 (71) 97 (71) 77 (57)	-	

Table 8. Conditions of SCC Test.

Sample	Weld metal: 2.25Cr-1Mo steel PWHT: 600°C (1112°F), 10h
Specimen	U-bend shape -Base metal -HAZ -Weld metal
Environment	NaCl solution -10ppm -100ppm
Temperature	80 °C (353°F)
Time	Max. 1000h

Welding and Heat Treatment for the Rotor Disk

An actual rotor was welded and heat treated for a real scale test. Figure 13 shows the appearance of a welded disk. 2.25Cr-1Mo was welded 60 mm (2.36 inches) in height by GTAW. Welding speed was kept constant to prevent bowing of the rotor shaft.

Local heating was applied for the PWHT. Layout of the heater was decided based on the result of a finite element analysis to reduce the thermal stress around the edge of the heating zone due to temperature distribution. Figure 14 shows the schematic view of the heater layout. The rotor was suspended vertically during heating to avoid bowing due to the influence of gravity on the horizontal rotor layout.

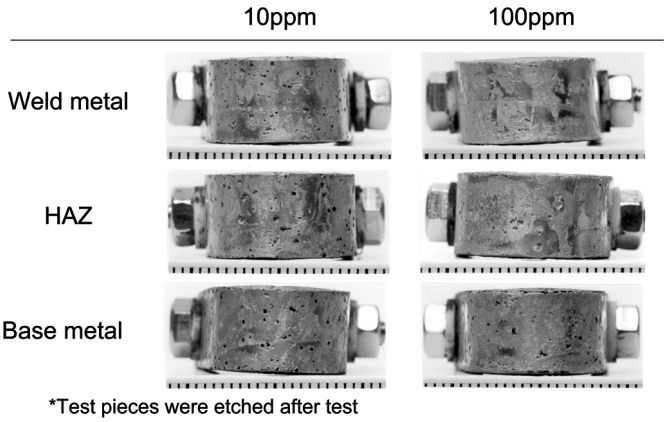

Figure 12. Surface of Specimens after 1000 Hours in NaCl Solution.

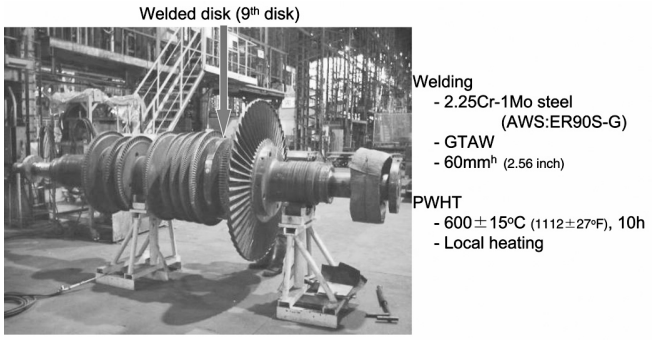

Figure 13. Welded Disk on Real Scale Test.

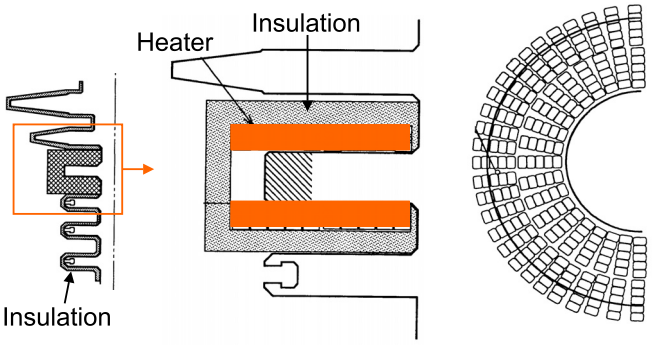

Figure 14. Heater Layout on Local PWHT for Welded Disk.

Evaluation of the Welded Rotor

Deformation

Measurement was performed for bowing of the shaft and other deformations due to welding and PWHT. No unfavorable deformation was found.

Welding Defects

The welded disk was inspected by ultrasonic testing. Defects exceeding the criterion [1.6 mm (.06 inch) in diameter] were not found. According to the analysis of fracture mechanics, the critical defect size for cracking is much larger then the criteria. Therefore, it can be concluded that any defects in the weld were small enough to prevent fractures.

Residual Stress

Figure 15 shows the appearance of the residual stress measurement. A strain gauge was attached to a square weld metal area, and a groove of 1 mm (.04 inch) in depth was cut around this area.

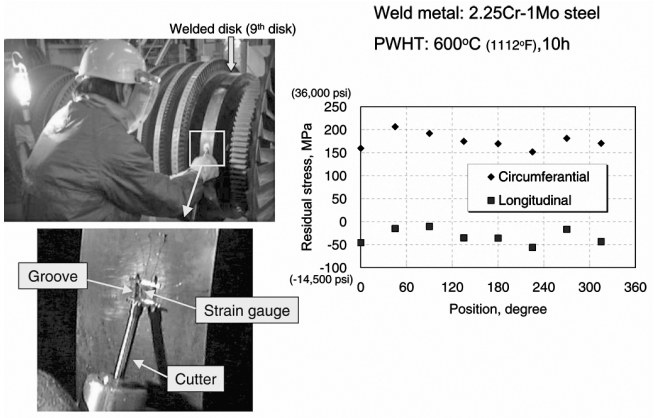

Figure 15. Residual Stress Measurement for Repaired Disk.

Measured strain after cutting was translated into the released residual stress. Measured residual stress was around 200 MPa (tension) in a circumferential direction. This corresponds to the target value required to prevent SCC and the value estimated through the finite element analysis.

Mechanical Properties

Hardness on the surface of the weld metal was measured. Figure 16 indicates the measured hardness. The measured hardness of 240 to 270 HV is almost the same as that of the final bead on the laboratory test piece heated at 600°C (1112°F) as shown in Figure 10. Therefore, it can be estimated that the hardness of HAZ was also reduced within 350 HV.

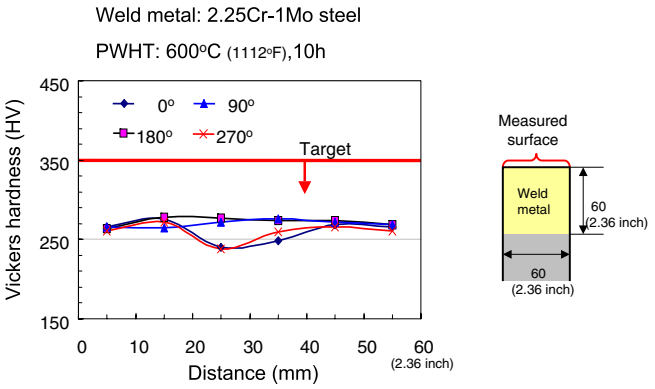

Figure 16. Hardness Distribution on Real Scale Disk.

NUMERICAL ANALYSIS

A finite element analysis was performed to set the optimum heater layout at local PWHT. Temperature distribution and thermal stress by elastic analysis were estimated through a heating process that included heating and cooling. Heater layout was adjusted to maintain a target thermal stress of less than 200 MPa. Analysis was performed for the heating of both the disk and the shaft.

Temperature and Stress Distribution on the Post Weld Heat Treatment Area of the Disk

Figure 17 shows the temperature distribution at the start of temperature hold after heating and the temperature change at each spot for positioned heaters. The temperature at the root of the heated disk and adjacent disks was less than 450°C (842°F). Therefore, temperature at the root of the disk should be maintained at more than 450°C (842°F) to satisfy the target residual stress.

Figure 18 shows the distribution of circumferential stress around the heated disk at the start of temperature hold. Circumferential

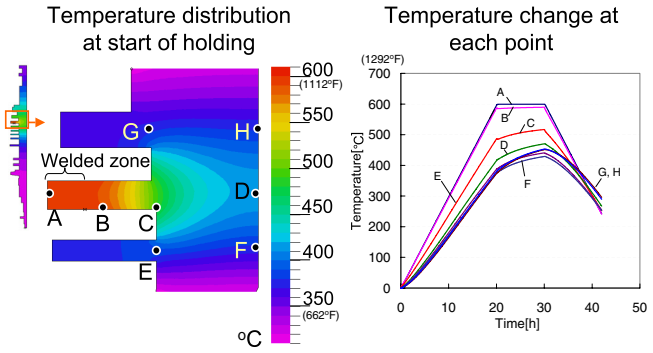

Figure 17. Estimated Temperature Distribution on Local PWHT for Disk.

stress is around −200 MPa on the weld metal. This means that the weld metal is compressed by the disk during heating. This stress is turned into tensile stress after cooling down. It is presumed that the compression stress during heating changes into tensile stress by creep deformation.

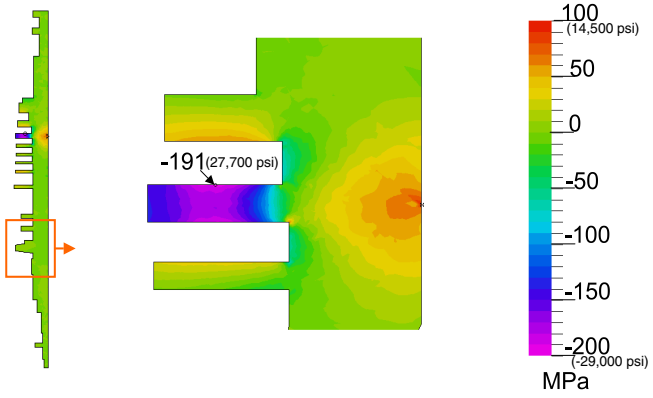

Figure 18. Estimated Circumferential Stress Distribution on Local PWHT for Disk.

Temperature and Stress Distribution of Post Weld Heat Treatment for the Shaft Portion

Figure 19 shows the temperature distribution at the start of temperature hold and the temperature change at each spot for positioned heaters that satisfy the uniform temperature on the whole surface of the weld metal. The center of the shaft's heated portion is more than 500°C (932°F). This means there is a higher possibility of unfavorable deformation by welding of the shaft and PWHT than that for the disk.

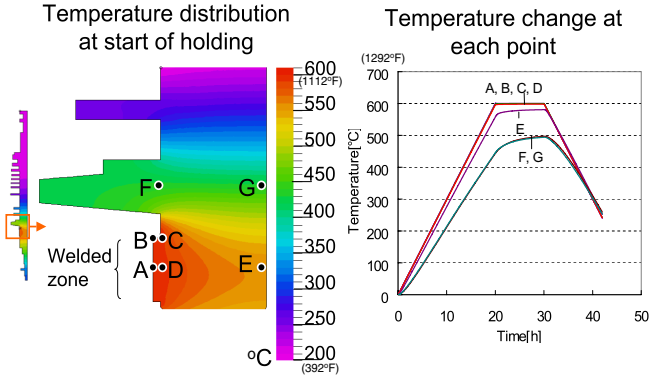

Figure 19. Estimated Temperature Distribution on Local PWHT for Shaft.

Figure 20 shows the distribution of circumferential stress around the heated shaft at the start of temperature hold. The stress around weld metal is low and the compressive stress is 75 MPa maximum in a circumferential direction around the edge of the heater. Therefore, it can be determined that the residual tensile stress on the shaft is lower than that on the disk. Bending residual stress around 80 MPa can be estimated on the disk adjacent to the heated portion. This is almost the same as that on the shaft.

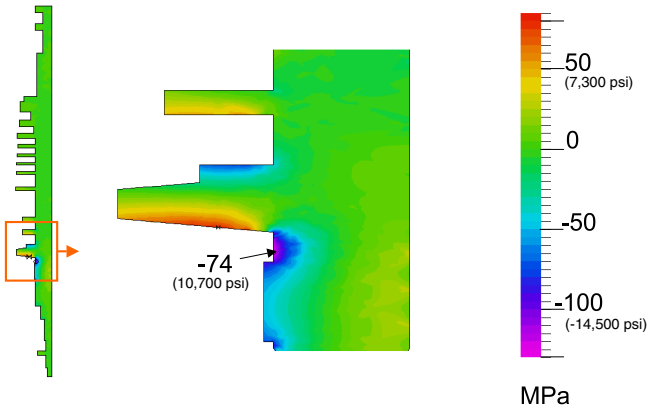

Figure 20. Estimated Circumferential Stress Distribution on Local PWHT for Shaft.

TYPICAL REPAIR EXPERIENCE

Experience in overlay welding for repairs is listed in Table 9. These overlay welds were performed in emergency cases. In considering rotor materials and the required strength, overlay welding was applied to a portion of blade root grooves and rotor disks by selecting suitable weld metals. In this paper, two typical repair experiences for mechanical drive turbines are introduced.

Table 9. Application of Rotor Overlay Welding.

No.	Use	Welded Part	Rotor Materials	Method
1	Ship	Root Groove (Partially)	Ni Cr Mo V	Overlay Welding
2	Power Generation	Root Groove (Partially)	Cr Mo V	Removal of Cracks Overlay Welding
3	Power Generation	Disk Side Plane (Circumference)	2.5Ni Cr Mo V	Overlay Welding
4	Power Generation	Whole Root Groove (Circumference)	—	Removal of the Whole Root Groove Overlay Welding
5	Mechanical Driver	Rotor Disk LP Section (1 Stage)	1.25Ni Cr Mo V	Removal of Damaged Disk Overlay Welding
6	Mechanical Driver	Rotor Disk HP and LP Section (4 Stages)	1.25Ni Cr Mo V	Removal of Damaged Disks Overlay Welding

Welding Repair for a Large Rotor

First, Figure 21 shows the case for a large rotor in a charge gas compressor drive steam turbine at an ethylene plant. The ninth stage disk of this turbine had heavy frictional contact with the diaphragm, and the blades and one side of the disk were damaged. The damaged portion was cut off and repaired successfully based on the results of the above laboratory test and analysis. Figure 22 shows hardness check results in the repair process used to confirm that the welding conditions are the same as in the test results.

Welding Repair for High-Speed Rotor

Second, as explained in the catastrophic damage of Figure 4 and Figure 5, the case for a high-speed machine is explained in detail. All stages of this rotor were damaged; thus it was necessary to repair all stages. However, it was also necessary to start the plant very quickly, and the time for repair was limited. In discussion with the customer regarding minimum required power in the plant, turbine performance and blade strengths of each stage were decided upon with the customer, and as a result, the number of stages were reduced and heat drop distribution was changed for the LP section. Figure 23 shows the condition of welding repair on the rotor disks. Figure 24 shows rotor residual warpage check after welding was completed. Rotor residual warpage after welding and final machining were within the criteria of 0.005 mm (.0002 inch), and the blades for each stage were assembled as shown in Figure 25.

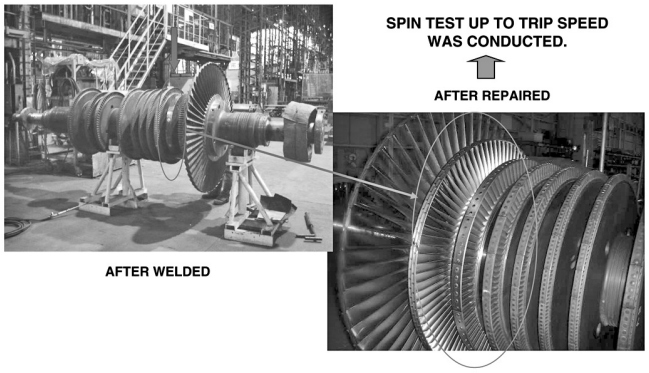

Figure 21. Welding of the Rotor Disk.

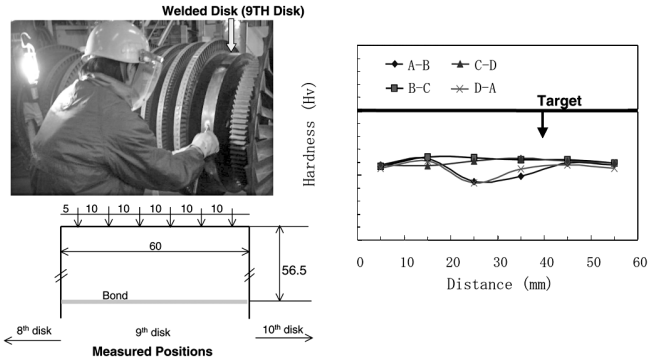

Figure 22. Hardness of the Welded Metal for the Actual Rotor.

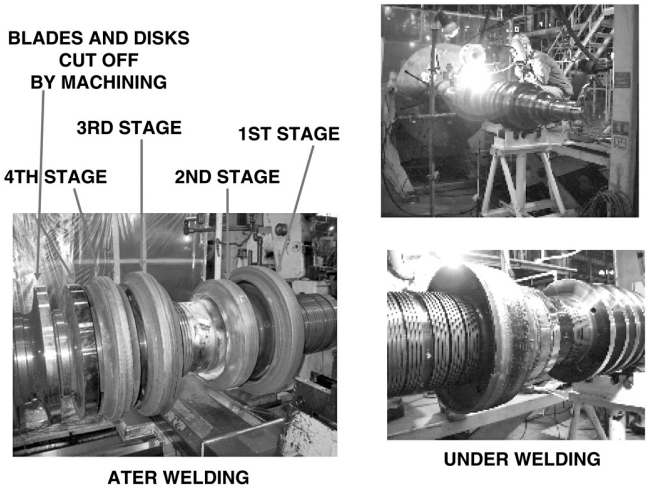

Figure 23. Welding Repair of Rotor Disks.

Figure 26 shows the comparison between the turbine performance curves at the original 9555 kW and after repairs at 6700 kW, with the number of stages reduced by cutting off the last fifth,

Figure 24. Rotor Residual Warpage Check.

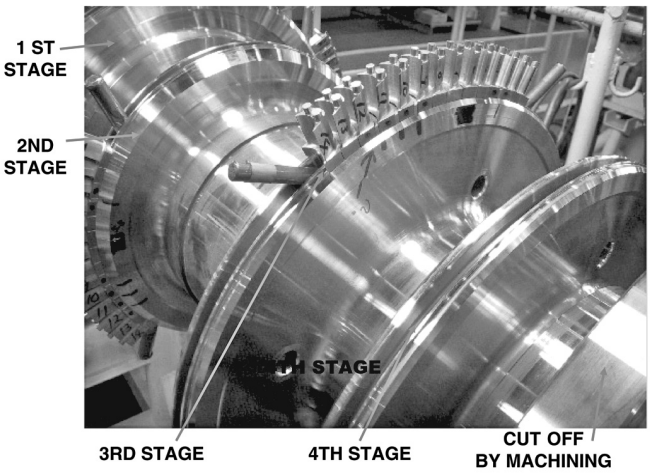

Figure 25. Blade Assembly after Welding Repair.

sixth, and seventh stages. Blades and diaphragm strengths were checked and exhaust vacuum pressure was limited. This repaired and revived the rotor of the extraction condensing turbine, and it was actually placed back into the casing and operated successfully at a condition with low vibration and full load for three months until the new rotor was prepared.

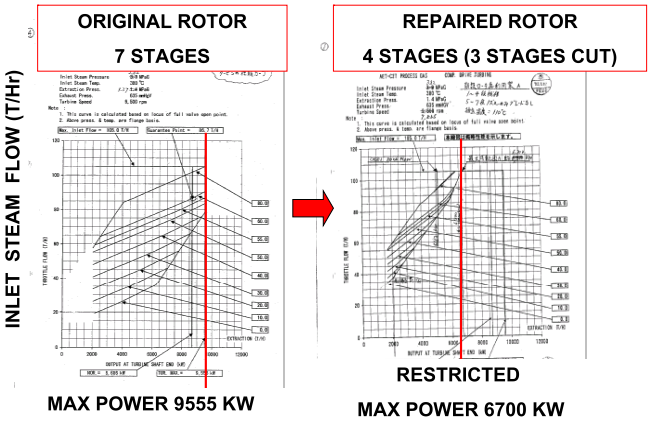

Figure 26. Actual Operation of Repaired Rotor.

CONCLUSIONS

This paper introduces typical steam turbine engine damage modes and causes, and actual experiences in repairing and reviving catastrophically damaged turbine rotors through special welding procedures, based on risk analysis for rotor repair from a systematic viewpoint.

Root cause analysis in the catastrophic failure process is explained, regarding the integrated control system for governor control and backup system. The practical repair techniques are developed based on element tests to find optimized welding conditions and detailed strength calculation to confirm the integrity, and heat transfer analysis for proper heat treatment process conditions.

These basic procedures are discussed to show useful data. The case study for this optimization is discussed by showing thermodynamic calculation, performance, and repair schedule. Finally, this turbine was uniquely modified in order to balance required power and repair time, in order to quickly restart the plant in an emergency case, to acquire customer satisfaction. The revived extraction condensing turbine rotor was placed back into the casing and operated successfully at full load.

REFERENCES

Speidel, M. O. and Bertilsson, J. E., 1984, International Brown Boveri Symposium on Corrosion in Power Generating Equipment, p. 331.

ACKNOWLEDGEMENT

The authors gratefully wish to acknowledge the following individuals for their contribution and technical assistance in analyzing and experiments: O. Isumi and M. Wakai of Mitsubishi Heavy Industries Ltd.